

Stable second-order formulation of Einstein's equations

By K. Mattsson

1. Motivation and objectives

This project is focused on the numerical solutions of Einstein's equations, which describe processes such as binary black holes and neutron star collisions. The outcome of this kind of simulation is considered to be crucial for the successful detection and interpretation of gravitational waves, expected to be measured by laser interferometers such as LIGO, GEO600, LISA and others. In turn, measurement of gravitational waves will constitute a strong, direct verification of Einstein's theory, and open a new window to the universe. The construction of these numerical solutions requires large-scale computations and research on a variety of physical, mathematical, numerical and scientific computing issues. The simulation of black holes has proved to be a difficult computational problem.

In the harmonic description of general relativity, the principal part of Einstein's equations reduces to 10 curved space wave equations for the component of the space-time metric. Although these equations can be reduced to first-order symmetric hyperbolic form (Fisher & Marsden 1972), this has the disadvantage of introducing auxiliary variables with their constraints and boundary conditions. The reduction to first-order form is also less attractive from a computational point of view considering the efficiency and accuracy (Kreiss *et al.* 2002; Mattsson & Nordström 2006). The reasons for solving the equations on first-order form are most likely related to the maturity of CFD, which has evolved during the last 40 years. Many of the stability issues for first-order hyperbolic problems have already been addressed.

For wave-propagation problems, the computational domain is often large compared to the wavelengths, which means that waves have to travel long distances over long times. As a result, high-order accurate time marching methods, as well as high-order spatially accurate schemes (at least third-order) are required. Such schemes, although they might be G-K-S stable (Gustafsson *et al.* 1972) (convergence to the true solution as $\Delta x \rightarrow 0$), may exhibit a non-physical growth in time (Carpenter *et al.* 1994) for realistic mesh sizes. It is therefore important to devise schemes that do not allow a growth in time that is not called for by the differential equation. Such schemes are called strictly (or time) stable.

Deriving time-stable numerical simulations of Einstein's equations on second-order form has proven to be a very difficult task (Szilagy1 *et al.* 2005; Calabrese 2005), especially for higher order discretizations. The major difficulty is the treatment of the boundaries. This situation is modeled by a 1-D model problem (3.1) that captures most of the stability issues without introducing unnecessary notation.

In this paper it will be shown how time-stability of the model problem can be obtained by employing the newly developed narrow-stencil summation by parts (SBP) operators, SBP preserving artificial dissipation (Mattsson *et al.* 2004), and the Simultaneous Approximation Term (SAT) method (Carpenter *et al.* 1994) for implementing the physical boundary conditions. This technique can be extended to address the full 3-D problem.

In Section 2 we discuss the SBP property for the first- and second-derivative difference

operators, and show an important relationship between the first- and second-derivative SBP operators, referred to as *full compatibility*. A 1-D model for Einstein's equations is introduced in Section 3, and we show how to combine the SAT method and the SBP operators to obtain stable finite-difference approximations using the energy method in combination with an eigenvalue analysis. Conclusions and future work are presented in Section 4.

2. Definitions

The 2-D and 3-D schemes are constructed using 1-D SBP finite-difference operators (see Kreiss & Scherer (1974); Strand (1994); Mattsson & Nordström (2004)). We begin with a short description and some definitions.

Let the inner product for real-valued functions $u, v \in L^2[0, 1]$ be defined by $(u, v) = \int_0^1 u v w dx$, $w(x) > 0$, and let the corresponding norm be $\|u\|_w^2 = (u, u)$. The domain ($0 \leq x \leq 1$) is discretized using $N+1$ equidistant grid points,

$$x_i = i h, \quad i = 0, 1, \dots, N, \quad h = \frac{1}{N}.$$

The approximate solution at grid point x_i is denoted v_i , and the discrete solution vector is $v^T = [v_0, v_1, \dots, v_N]$. Similarly, we define an inner product for discrete real-valued vector functions $u, v \in \mathbf{R}^{N+1}$ by $(u, v)_H = u^T H v$, where $H = H^T > 0$, with the corresponding norm $\|v\|_H^2 = v^T H v$. The following vectors will be frequently used:

$$e_0 = [1, 0, \dots, 0]^T, \quad e_N = [0, \dots, 0, 1]^T. \quad (2.1)$$

2.1. Narrow-diagonal SBP operators

To introduce narrow-diagonal SBP operators, we present the following definition:

Definition 2.1. *An explicit p th-order accurate finite-difference scheme with minimal stencil width of a Cauchy problem is called a p th-order accurate narrow stencil.*

We say that a scheme is explicit if no linear system of equations need to be solved to compute the difference approximation. Spatial Padé discretizations (Lele 1992) are often referred to as “compact schemes”. The approximation of the derivative is obtained by solving a tri- or penta-diagonal system of linear equations at every time step. Hence, if written in explicit form, Padé discretizations lead to full-difference stencils, similar to spectral discretizations.

Consider the hyperbolic scalar equation $u_{tt} + u_{tx} = 0$ (excluding the boundary condition). Multiplying by u_t and integrating by parts (referred to as “the energy method”) lead to

$$\frac{d}{dt} \|u_t\|^2 = -(u_t, u_{tx}) - (u_{tx}, u_t) = -u_t^2|_0^1, \quad (2.2)$$

where $u_t^2|_0^1 \equiv u_t^2(x=1) - u_t^2(x=0)$.

Definition 2.2. *A difference operator $D_1 = H^{-1}Q$ approximating $\partial/\partial x$, using a p th-order accurate narrow stencil, is said to be a p th-order accurate narrow-diagonal first-derivative SBP operator, if H is diagonal and positive definite, and $Q + Q^T = B = \text{diag}(-1, 0, \dots, 0, 1)$.*

As an example of its use, consider the semi-discretization of $u_{tt} + u_{tx} = 0$, which is

$v_{tt} + D_1 v_t = 0$. Multiplying by $v_t^T H$ from the left and adding the transpose lead to

$$\frac{d}{dt} \|v_t\|_H^2 = -(v_t, H^{-1} Q v_t)_H - (H^{-1} Q v_t, v_t)_H = -v_t^T (Q + Q^T) v_t = (v_t)_0^2 - (v_t)_N^2. \quad (2.3)$$

Estimate (2.3) is the discrete analog of Eq. 2.2.

For hyperbolic problems on second-order form, we need an SBP operator for the second derivative. Consider the wave equation

$$u_{tt} = u_{xx}. \quad (2.4)$$

Multiplying Eq. 2.4 by u_t and integrating by parts lead to

$$\frac{d}{dt} (\|u_t\|^2 + \|u_x\|^2) = 2 u_t u_x|_0^1. \quad (2.5)$$

Definition 2.3. Let $D_2 = H^{-1}(-M + BS)$ approximate $\partial^2/\partial x^2$, using a p th-order accurate narrow stencil. D_2 is said to be a p th-order accurate narrow-diagonal second-derivative SBP operator, if H is diagonal and positive definite, M is symmetric and positive semi-definite, S approximates the first-derivative operator at the boundaries and $B = \text{diag}(-1, 0, \dots, 0, 1)$.

(High-order accurate narrow-diagonal second-derivative SBP operators were constructed in Mattsson & Nordström (2004).) An example of its use is the semi-discretization $v_{tt} = D_2 v$ of Eq. 2.4. Multiplying by $v_t^T H$ and adding the transpose lead to

$$\frac{d}{dt} (\|v_t\|_H^2 + v^T M v) = 2(v_t)_N (B S v)_N + 2(v_t)_0 (B S v)_0. \quad (2.6)$$

Estimate (2.6) is a discrete analog of Eq. 2.5. Obtaining energy estimates for schemes utilizing both D_1 and D_2 requires that both are based on the same norm H .

The following definition is central to the present study:

Definition 2.4. Let D_1 and D_2 be p th-order accurate narrow-diagonal first- and second-derivative SBP operators. If $D_2 = H^{-1}(-D_1^T H D_1 - R^{(p)} + B D_1)$, and the remainder $R^{(p)}$ is positive semi-definite, D_1 and D_2 are called fully compatible.

Employing the first-derivative SBP operator twice (leading to a wide stencil) yields $D_1 D_1 = H^{-1}(-D_1^T H D_1 + B D_1)$. Hence, for fully compatible p th-order accurate SBP operators, the following property holds: $D_2 = D_1 D_1 - H^{-1} R^{(p)}$, where $R^{(p)}$ is symmetric and positive semi-definite. Fully compatible SBP operators for the sixth-order case are presented in Section 5.

For the Cauchy problem, i.e., disregarding the one-sided boundary closures of the SBP operators, the following relations for the remainders $R^{(p)}$ ($p = 2, 4, 6, 8$) hold:

$$\begin{aligned} -R^{(2)} &= -\frac{h^3}{4} D_4 \\ -R^{(4)} &= +\frac{h^5}{18} D_6 - \frac{h^7}{144} D_8 \\ -R^{(6)} &= -\frac{h^7}{80} D_8 + \frac{h^9}{600} D_{10} - \frac{h^{11}}{3600} D_{12} \\ -R^{(8)} &= +\frac{h^9}{350} D_{10} - \frac{h^{11}}{2520} D_{12} + \frac{h^{13}}{14700} D_{14} - \frac{h^{15}}{78400} D_{16}. \end{aligned} \quad (2.7)$$

$D_{2n} = (D_+ D_-)^n$ is an approximation of $\frac{d^{2n}}{dx^{2n}}$. For example, $(D_+ D_- v)_j = (v_{j+1} - 2v_j + v_{j-1})/h^2$ is the second-order accurate narrow second-derivative finite-difference approximation.

The action of a derivative of order n on a pure Fourier mode $e^{i\omega x}$, results in $(i\omega)^n e^{i\omega x}$. The second derivative, for example, gives $-\omega^2 e^{i\omega x}$. Consider the same Fourier mode on a grid over $[-1, 1]$ with grid spacing h . The Fourier mode defined on the grid is given by $\hat{u}^T = [e^{i\omega x_1}, e^{i\omega x_2}, \dots, e^{i\omega x_N}]$, assuming periodicity ($\hat{u}_1 = \hat{u}_N$). It is convenient to introduce a scaled wavenumber $k = \omega h$, where $k \in [0, \pi]$. The Fourier mode for the wavenumber $k = \pi$, is $\hat{u}^T = [1, -1, 1, \dots, -1, 1]$ (the highest frequency that can exist on the grid). It can be shown that a centered, second-order accurate undivided difference operator of order n , applied to a Fourier mode results in $\tilde{D}_n \hat{u} = (2i)^n \hat{u} \sin^n(\frac{k}{2})$. This shows that $-R^{(p)}$ constitutes only dissipative terms.

Definition 2.5. Let $R^{(p)}$ be the remainder for the Cauchy problem, given by Eq. 2.7. Let $\tilde{R}^{(p)}$ be defined as the minimal stencil, such that $\tilde{R}^{(p)} \hat{u} \geq R^{(p)} \hat{u}$. Then we say that $\tilde{R}^{(p)}$ dominates $R^{(p)}$.

For the Cauchy problem $\tilde{R}^{(p)}$ ($p = 2, 4, 6, 8$) is given by:

$$\tilde{R}^{(2)} = \frac{h^3}{4} D_4, \quad \tilde{R}^{(4)} = -\frac{h^5}{12} D_6, \quad \tilde{R}^{(6)} = \frac{17h^7}{720} D_8, \quad \tilde{R}^{(8)} = -\frac{2h^9}{315} D_{10}. \quad (2.8)$$

Definition 2.6. Let $R^{(p)}$ be the remainder for the boundary-value problem. Let $\tilde{R}^{(p)}$ be defined as the minimal stencil, such that the eigenvalues of $(\tilde{R}^{(p)} - R^{(p)})$ are non-negative. Then we say that $\tilde{R}^{(p)}$ dominates $R^{(p)}$.

For the boundary-value problem, an eigenvalue analysis results in

$$\tilde{R}^{(2)} = 1.00 \frac{h^3}{4} D_2^T D_2, \quad \tilde{R}^{(4)} = 1.06 \frac{h^5}{12} D_3^T D_3, \quad \tilde{R}^{(6)} = 2.94 \frac{17h^7}{720} D_4^T D_4, \quad (2.9)$$

where $(D_{2,3,4,5})v$ are consistent approximations of u_{xx} , u_{xxx} , u_{xxxx} and u_{xxxxx} , respectively (see Mattsson *et al.* (2004)).

3. The linear 1-D problem

We consider

$$u_{tt} - (au_x)_t - (au_t)_x - ((b - a^2)u_x)_x = 0 \quad (3.1)$$

to be a 1-D model of Einstein's equations, with the assumption that b is positive. We note that (3.1) can be written as

$$(\partial/\partial t - \lambda_1 \partial/\partial x)(\partial/\partial t - \lambda_2 \partial/\partial x)u = 0, \quad (3.2)$$

where $\lambda_{1,2} = a \pm \sqrt{b}$, indicating the characteristics. The model (3.1) was analyzed in Szilagyl *et al.* (2005), using a second order non-SBP discretization. Here we want to extend the analysis i) to higher-order, and ii) to introduce an energy-stable boundary treatment employing SBP operators and the SAT technique.

The case where $c \equiv (b - a^2) < 0$ in (3.1) requires special attention to obtain a valid energy estimate, and hence a stable numerical approximation. To simplify the analysis (without restriction to the continuous problem) we study the constant coefficient problem

$$u_{tt} - 2au_{xt} - cu_{xx} = 0, \quad (3.3)$$

(obtained by linearizing and freezing the coefficients in (3.1)). Artificial boundaries are introduced at $x = 0, 1$. The energy method is used to derive suitable boundary conditions. The regular technique (see Section 2), multiplying Eq. 3.3 by u_t and integrating by parts

lead to

$$\frac{d}{dt}E_0 = 2u_t(au_t + cu_x)|_0^1, \quad (3.4)$$

where

$$E_0 = (\|u_t\|^2 + c\|u_x\|^2). \quad (3.5)$$

This is a valid energy for $c \geq 0$, but not for $c < 0$. To obtain an energy for $c < 0$, we multiply Eq. 3.3 by $u_t - au_x$ and integrate by parts to obtain

$$\frac{d}{dt}E_1 = \left(\frac{\lambda_1}{2}(u_t - \lambda_2 u_x)^2 + \frac{\lambda_2}{2}(u_t - \lambda_1 u_x)^2 \right) |_0^1, \quad (3.6)$$

where

$$E_1 = (\|u_t - au_x\|^2 + b\|u_x\|^2). \quad (3.7)$$

This is a valid energy for any c . The problem is to devise a stable and accurate narrow-stencil approximation to Eq. 3.3, including the boundary treatment.

To obtain a well-posed problem we close Eq. 3.3 with appropriate boundary conditions (depending on the sign of c). With no restriction we assume that $a > 0$ (if $a < 0$ the number of boundary conditions that needs to be specified at each boundary is reversed). We have three different scenarios: $c > 0$, $c = 0$ and $c < 0$.

3.1. Case 1, $c > 0$

If $c > 0$, the energy method using E_0 Eq. 3.4 or E_1 Eq. 3.6 (or by studying the direction of the characteristics Eq. 3.2) shows that we need to specify one boundary condition at each boundary. The characteristic boundary conditions (CBC) are given by

$$\begin{aligned} L_0 u &= u_t - \lambda_1 u_x = g_0 & x &= 0 \\ L_1 u &= u_t - \lambda_2 u_x = g_1 & x &= 1. \end{aligned} \quad (3.8)$$

To simplify the analysis we assume that the boundary data is homogeneous. (The analysis holds for inhomogeneous data, but introduces unnecessary notation.) The energy method applied to Eq. 3.3 with the CBCs (3.8) leads to

$$\frac{d}{dt}E_0 = -2\sqrt{b}(u_0)_t^2 - 2\sqrt{b}(u_1)_t^2, \quad (3.9)$$

or

$$\frac{d}{dt}E_1 = -\frac{2\sqrt{b}}{\lambda_1}(u_0)_t^2 + \frac{2\sqrt{b}}{\lambda_2}(u_1)_t^2. \quad (3.10)$$

A semi-discretization of (3.1) using narrow-diagonal SBP operators D_1 , D_2 , and the SAT method to impose the CBCs (3.8), can be written as

$$v_{tt} - 2aD_1 v_t - cD_2 v = SAT_0 + SAT_1. \quad (3.11)$$

The penalty terms in Eq. 3.11 are given by $SAT_0 = \tau_0 H^{-1} e_0 (L_0^T v - g_0)$ and $SAT_1 = \tau_1 H^{-1} e_N (L_1^T v - g_1)$. The discrete versions of the CBCs (3.8) are given by

$$\begin{aligned} L_0^T v &= v_t - \lambda_1 (Sv)_0 = g_0 \\ L_1^T v &= v_t - \lambda_2 (Sv)_N = g_1. \end{aligned} \quad (3.12)$$

Lemma 3.1. *The scheme (3.11) with homogeneous data is stable if $c > 0$, $\tau_0 = \lambda_2$ and $\tau_1 = -\lambda_1$ hold.*

Proof. Let $g_0 = g_1 = 0$. Multiplying Eq. 3.11 by $v_t^T H$ from the left and adding the transpose lead to

$$\begin{aligned} \frac{d}{dt}(\|v_t\|_H^2 + cv^T Mv) &= 2(v_0)_t^2(-a + \tau_0) + 2(v_N)_t^2(a + \tau_1) \\ &\quad - 2(v_0)_t(Sv)_0(c + \tau_0\lambda_1) + 2(v_N)_t(Sv)_N(c - \tau_1\lambda_2), \end{aligned}$$

assuming that M is symmetric. To obtain an energy estimate requires that M is positive semi-definite, $\tau_0 = -c/\lambda_1 \equiv \lambda_2$ and $\tau_1 = c/\lambda_2 \equiv -\lambda_1$ hold. This leads to

$$\frac{d}{dt}(\|v_t\|_H^2 + cv^T Mv) = -2\sqrt{2}(v_0)_t^2 - 2\sqrt{2}(v_N)_t^2,$$

which exactly mimics the continuous estimate (3.9). By assumption, D_2 is a narrow-stencil SBP operator, meaning that M is both symmetric and positive semi-definite. \square

3.2. Case 2, $c = 0$

If $c = 0$, Eq. 3.3 reduces to a hyperbolic first-order problem. In this case $\lambda_2 = 0$ and $\lambda_1 > 0$, meaning that we need to specify only one boundary condition $u_t = g$, at $x = 0$. The energy method applied to Eq. 3.3 leads to

$$\frac{d}{dt}\|u_t\|^2 = 2a(g^2 - (v_N)_t^2). \quad (3.13)$$

A semi-discretization of (3.1) is given by

$$v_{tt} - 2aD_1v_t = -2a\tau H^{-1}e_0((v_0)_t - g). \quad (3.14)$$

The energy method applied to Eq. 3.14 leads to

$$\frac{d}{dt}\|v_t\|_H^2 = 2a\left(\frac{\tau^2}{2\tau-1}g^2 - (v_0)_t^2 - (2\tau-1)\left((v_0)_t - \frac{\tau}{2\tau-1}g\right)^2\right).$$

An energy estimate exists for $\tau > 1/2$. The choice $\tau = 1$ yields

$$\frac{d}{dt}\|v\|_H^2 = 2a(g^2 - (v_0)_N^2 - ((v_0)_t - g)^2),$$

which is a discrete analog of the integration by parts formula Eq. 3.13 in the continuous case, where the extra term $((v_0)_t - g)^2$ introduces a small additional damping.

3.3. Case 3, $c < 0$

If $c < 0$, an energy estimate can be shown in the energy E_1 Eq. 3.7, which is obtained by multiplying Eq. 3.3 with $u_t - au_x$ and integrating by parts. For the semi-discrete approximation, this complicates the imposition of boundary conditions using SAT. We begin by studying this case using only a first-derivative SBP operator, to show that the stability problem is not restricted to the narrow-stencil approximation (although the narrow-stencil approximation introduces some additional complications, shown later in this section).

With $c < 0$ we need to specify two boundary conditions at $x = 1$. No boundary conditions should be given at $x = 0$ (with $a < 0$ it is the other way around, i.e., two boundary conditions at $x = 0$). Well-posed boundary conditions are given by

$$\begin{aligned} L_{11}u &= u_t = g_{11} & x &= 1 \\ L_{12}u &= u_x = g_{12} & x &= 1. \end{aligned} \quad (3.15)$$

A semi-discretization of (3.1) using only the first-derivative SBP operator D_1 , and the SAT method to impose the boundary conditions Eq. 3.15, can be written as

$$v_{tt} - 2aD_1v_t - cD_1D_1v = SAT_2 . \quad (3.16)$$

The penalty term in Eq. 3.16 is given by $SAT_2 = \tau_{11}H^{-1}e_N(L_{11}v - g_{11}) + \tau_{12}H^{-1}e_N(L_{12}v - g_{12})$. The discrete versions of the boundary conditions (3.15) are given by

$$\begin{aligned} L_{11}^T v &= (v_N)_t = g_{11} \\ L_{12}^T v &= (D_1v)_N = g_{12} . \end{aligned} \quad (3.17)$$

Let $g_{11} = g_{12} = 0$ to simplify the notation. Multiplying Eq. 3.16 by $v_t^T H - av^T Q^T$ from the left and adding the transpose lead to

$$\frac{d}{dt}(E_1)_H = w_N^T R_N w_N - w_0^T R_0 w_0 ,$$

introducing the discrete energy

$$(E_1)_H = (\|v_t - aD_1v\|_H^2 + b\|D_1v\|_H^2) . \quad (3.18)$$

Here $w_{0,N}^T = [(v_{0,N})_t, (D_1v)_{0,N}]$ and

$$R_N = \begin{bmatrix} a + \tau_{11} & c - a\tau_{11} + \tau_{12} \\ c - a\tau_{11} + \tau_{12} & -ac - 2a\tau_{12} \end{bmatrix}, \quad R_0 = \begin{bmatrix} a & c \\ c & -ac \end{bmatrix} .$$

Since R_0 is positive definite, stability follows if R_N can be made negative semi-definite by proper tuning of the penalty parameters τ_{11} and τ_{12} . However, it can be found (although not shown here) that R_N can not be made negative semi-definite with only these two penalties.

By introducing the auxiliary variable $w \equiv v_t$, Eq. 3.16 can be written

$$\begin{aligned} v_t &= w \\ w_t &= 2aD_1w + cD_1D_1v + SAT_2 , \end{aligned} \quad (3.19)$$

where $SAT_2 = \tau_{11}H^{-1}e_N(w_N - g_{11}) + \tau_{12}H^{-1}e_N((D_1v)_N - g_{12})$. The reason for introducing Eq. 3.19 is twofold: 1) We would like to employ a Runge-Kutta method to time-advance the semi-discrete problem, and 2) We need another penalty SAT_1 to turn R_N negative semi-definite. The new penalty term is given by $SAT_1 = \tau_{13}H^{-1}D_1^T e_N((D_1v)_N - g_{12})$ and is added to the first equation in Eq. 3.19, i.e., we obtain the modified problem

$$\begin{aligned} v_t &= w + SAT_1 \\ w_t &= 2aD_1w + cD_1D_1v + SAT_2 . \end{aligned} \quad (3.20)$$

This means that $w \neq v_t$. To obtain a hint of properly tuning the penalty parameters, we continue with the false assumption that $w = v_t$, in the second equation in Eq. 3.19. The energy method then leads to

$$\frac{d}{dt}(E_1)_H = w_N^T \tilde{R}_N w_N - w_0^T R_0 w_0 ,$$

where now

$$\tilde{R}_N = \begin{bmatrix} a + \tau_{11} & c - a\tau_{11} + \tau_{12} \\ c - a\tau_{11} + \tau_{12} & -ac - 2a\tau_{12} + 2\tau_{13} \end{bmatrix} .$$

Stability would then (under the false assumption) follow if \tilde{R} is negative semi-definite. By choosing

$$\tau_{11} = -a, \quad \tau_{12} = a\tau_{11} - c, \quad 2\tau_{13} = ac + 2a\tau_{12}, \quad (3.21)$$

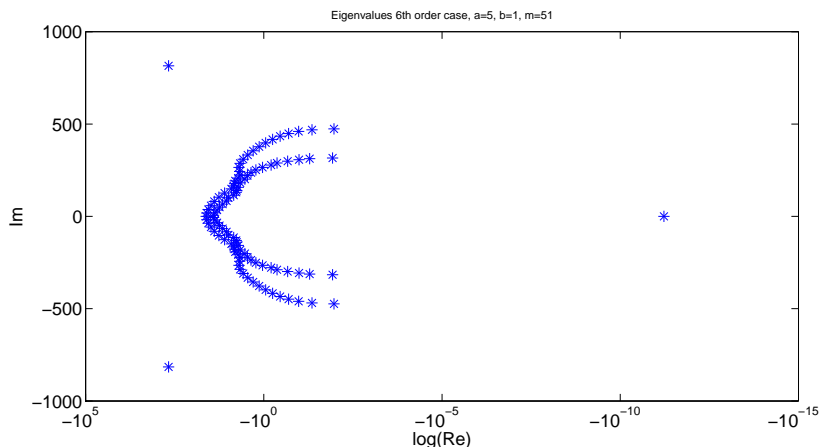


FIGURE 1. The eigenvalues to Eq. 3.20 using the sixth-order accurate operator, with $b = 1$, $a = 5$, $m = 51$. The penalty parameters are given by Eq. 3.22.

we obtain $\tilde{R}_N = \text{diag}(-a, 0)$. An eigenvalue analysis (not shown here) reveals that this particular choice does not lead to a time-stable approximation since we obtain small positive eigenvalues. This shows that the assumption is not valid and the energy method fails.

However, a more careful eigenvalue analysis (not shown here) shows that the following parameter choice

$$\tau_{11} = -a, \quad \tau_{12} = 2(c + a + b), \quad 3\tau_{13} = -h^2(a - b), \quad (3.22)$$

leads to a stable approximation. The eigenvalues to Eq. 3.20 using the sixth-order accurate D_1 operator (presented in Section 5), with $b = 1$, $a = 5$, $m = 51$, and the penalty parameters given by Eq. 3.22 is presented in Fig. 1. Our main focus is to derive stability conditions for a semi-discretization of (3.1) using narrow-diagonal SBP operators D_1 and D_2 . We will show that this can be done if 1) D_1 and D_2 are fully compatible, and 2) a suitable amount of artificial dissipation is added.

Consider the narrow-stencil approximation

$$\begin{aligned} v_t &= w + \tilde{S}\tilde{A}T_1 + \tilde{D}I_1 \\ w_t &= 2aD_1w + cD_2v + \tilde{S}\tilde{A}T_2 + \tilde{D}I_2, \end{aligned} \quad (3.23)$$

where

$$\begin{aligned} \tilde{S}\tilde{A}T_1 &= \tau_{13}H^{-1}S^T e_N((Sv)_N - g_{12}) \\ \tilde{S}\tilde{A}T_2 &= \tau_{11}H^{-1}e_N(w_N - g_{11}) + \tau_{12}H^{-1}e_N((Sv)_N - g_{12}), \end{aligned}$$

and

$$\begin{aligned} \tilde{D}I_1 &= c\sigma_1H^{-1}\tilde{R}^{(p)} + c\sigma_2H^{-1}D_1^T\tilde{R}^{(p)}D_1 \\ \tilde{D}I_2 &= c\sigma_3H^{-1}\tilde{R}^{(p)}. \end{aligned}$$

Possible formulations of $\tilde{R}^{(p)}$ are given in Eq. 2.9.

Lemma 3.2. *The p th-order accurate scheme (3.23) is stable if Eq. 3.20 is stable, if D_1 and D_2 are fully compatible, and if $\sigma_1 = \sigma_2 = a$, $a\sigma_3 = 1$ hold.*

Proof. By multiplying the first row in Eq. 3.20 by $v^T H$ from the left and the second

row by $w^T H - av^T Q^T$ and adding the transpose, we obtain

$$\frac{d}{dt}(E_1)_H = BT,$$

where BT corresponds to the boundary terms. By assumption BT is non-positive. For fully compatible p th-order accurate SBP operators, the following property holds: $D_2 = D_1 D_1 - H^{-1} R^{(p)}$, where $R^{(p)}$ is positive semi-definite. This means that the energy method applied to Eq. 3.23 leads to

$$\frac{d}{dt}(E_1)_H = BT + cx^T Ax,$$

where

$$x = \begin{bmatrix} v \\ D_1 u \\ w \end{bmatrix}, \quad A = \begin{bmatrix} 2\sigma_1 \tilde{R}^{(p)} & a R^{(p)} & -R^{(p)} \\ a R^{(p)} & 2\sigma_2 \tilde{R}^{(p)} & -a R^{(p)} \\ -R^{(p)} & -a R^{(p)} & 2\sigma_3 \tilde{R}^{(p)} \end{bmatrix}.$$

Since $\tilde{R}^{(p)}$ dominates $R^{(p)}$, the matrix A is positive semi-definite if

$$\tilde{A} = \begin{bmatrix} 2\sigma_1 & a & -1 \\ a & 2\sigma_2 & -a \\ -1 & -a & 2\sigma_3 \end{bmatrix}$$

is positive definite, which is true if $\sigma_1 = \sigma_2 = a$, $a\sigma_3 = 1$ hold. \square

A more careful eigenvalue analysis (not presented here) reveals that we can use slightly less artificial dissipation to maintain time-stability. By using fully compatible SBP operators it is found that Eq. 3.23 is stable if $\sigma_2 = 0$ and $\sigma_1 = \sigma_3 = \alpha^{(p)}$ (we use p to denote different orders of accuracy), where

$$\alpha^{(2)} = \frac{h}{3}, \quad \alpha^{(4)} = \frac{h}{5}, \quad \alpha^{(6)} = \frac{h}{9}. \quad (3.24)$$

The eigenvalues of Eq. 3.23 using the fully compatible sixth-order accurate operators, with $b = 1$, $a = 10$, $m = 81$, the penalty parameters given by Eq. 3.22, and the dissipation parameters given by Eq. 3.24 are presented in Fig. 2.

4. Conclusions and future work

We have proven that narrow-stencil approximations of Einstein's equations written on second-order form are time-stable, if the first- and second-derivative finite difference operators are fully compatible, and a suitable amount of artificial dissipation is added. Our approach has been to use SBP operators and the SAT technique to enforce the boundary conditions.

The next step will be to simulate the full non-linear 3-D problem utilizing the same technique. To address many of the more challenging (interesting) problems, for example colliding black holes, will require a structured-unstructured hybrid discretization approach to efficiently capture all the relevant solution features. Unstructured volume-integrated SBP operators utilized in CDP were described in Ham *et al.* (2006). Hybrid coupling of unstructured finite volume and high-order finite difference discretizations for the compressible Navier-Stokes equations is described in Nordström *et al.* (2007), utilizing the SBP and SAT technique to guarantee a stable and accurate coupling. The Discontinuous Galerkin method is also a good candidate for the unstructured part, since it naturally utilizes SAT to couple the elements.

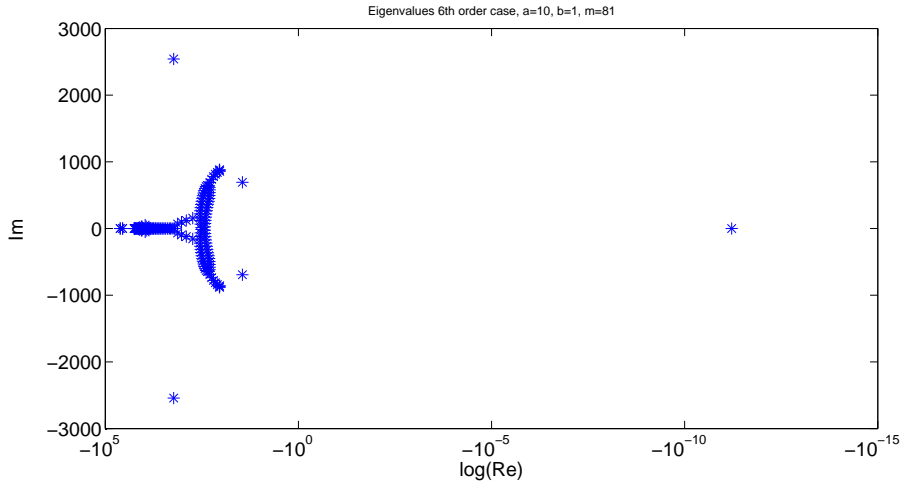


FIGURE 2. The eigenvalues to Eq. 3.23 using the sixth-order accurate operators, with $b = 1$, $a = 10$, $m = 81$.

Acknowledgments

This work is supported by the Advanced Scientific Computing Program of the United States Department of Energy.

5. Fully compatible SBP operators

The sixth order accurate fully compatible SBP operators are given below. The left boundary closure for the norm is given by:

$$H = \begin{bmatrix} \frac{7493827}{25401600} & 0 & 0 & 0 & 0 & 0 & 0 & 0 \\ 0 & \frac{5534051}{3628800} & 0 & 0 & 0 & 0 & 0 & 0 \\ 0 & 0 & \frac{104561}{403200} & 0 & 0 & 0 & 0 & 0 \\ 0 & 0 & 0 & \frac{260503}{145152} & 0 & 0 & 0 & 0 \\ 0 & 0 & 0 & 0 & \frac{43237}{103680} & 0 & 0 & 0 \\ 0 & 0 & 0 & 0 & 0 & \frac{514081}{403200} & 0 & 0 \\ 0 & 0 & 0 & 0 & 0 & 0 & \frac{3356179}{3628800} & 0 \\ 0 & 0 & 0 & 0 & 0 & 0 & 0 & \frac{25631027}{25401600} \end{bmatrix}$$

The left boundary closure of Q is given by:

$$\begin{array}{llll}
 q_{1,6} = \frac{49651253}{304819200} & q_{3,4} = \frac{9146267}{43545600} & q_{5,6} = \frac{906379}{43545600} & \\
 q_{1,7} = -\frac{111}{2000} & q_{3,5} = -\frac{140959}{777600} & q_{5,7} = \frac{654643}{3110400} & \\
 q_{1,8} = 0 & q_{3,6} = \frac{88913}{403200} & q_{5,8} = -\frac{1158071}{16934400} & \\
 q_{1,1} = -\frac{1}{2} & q_{2,3} = \frac{3554293}{21772800} & q_{3,7} = -\frac{2877293}{21772800} & q_{6,7} = \frac{59430457}{108864000} \\
 q_{1,2} = \frac{144243419}{217728000} & q_{2,4} = \frac{13951541}{21772800} & q_{3,8} = \frac{1810337}{60963840} & q_{6,8} = -\frac{5026031}{152409600} \\
 q_{1,3} = -\frac{100087}{6096384} & q_{2,5} = \frac{885133}{4838400} & q_{4,5} = \frac{31487}{145152} & q_{6,9} = -\frac{1}{60} \\
 q_{1,4} = -\frac{3349159}{16934400} & q_{2,6} = -\frac{54569873}{108864000} & q_{4,6} = \frac{3410983}{5443200} & q_{7,8} = \frac{30506159}{43545600} \\
 q_{1,5} = -\frac{8487881}{152409600} & q_{2,7} = \frac{24209}{129600} & q_{4,7} = -\frac{911107}{4838400} & q_{7,9} = -\frac{3}{20} \\
 & q_{2,8} = -\frac{1}{100} & q_{4,8} = -\frac{338713}{152409600} & q_{7,10} = \frac{1}{60}
 \end{array}$$

In the interior we have the skew-symmetric stencil $(Qv)_j = -\frac{1}{60}v_{j-3} + \frac{3}{20}v_{j-2} - \frac{3}{4}v_{j-1} + \frac{3}{4}v_{j+1} - \frac{3}{20}v_{j+2} + \frac{1}{60}v_{j+3}$. The left boundary closure of hM is given by

$$\begin{array}{ll}
 m_{1,1} = 1.2000574331050846310 & m_{4,4} = 4.4952269369790344874 \\
 m_{1,2} = -1.3493191282870869603 & m_{4,5} = -3.1817949974047985393 \\
 m_{1,3} = 0.070178887841234707543 & m_{4,6} = 1.0808018521848171469 \\
 m_{1,4} = 0.069590525249539236244 & m_{4,7} = -0.45961997566890306308 \\
 m_{1,5} = 0.067470908000967733967 & m_{4,8} = 0.086484339407630035030 \\
 m_{1,6} = -0.078177900310564991388 & m_{5,5} = 3.7441205742402132321 \\
 m_{1,7} = 0.020199274400825642921 & m_{5,6} = -2.2187585468457396535 \\
 m_{1,8} = 0 & m_{5,7} = 0.60169480955006113403 \\
 m_{2,2} = 2.3771262429420204291 & m_{5,8} = -0.082630532112906639616 \\
 m_{2,3} = -0.67656041117548601149 & m_{6,6} = 3.3035989548189179514 \\
 m_{2,4} = -0.17119675741265170011 & m_{6,7} = -1.7308643575320354723 \\
 m_{2,5} = -0.49114472782781516546 & m_{6,8} = 0.13993549254962779959 \\
 m_{2,6} = 0.41999078952455211907 & m_{6,9} = -\frac{1}{90} \\
 m_{2,7} = -0.11648186968013573680 & m_{7,7} = 2.6978965450148505391 \\
 m_{2,8} = 0.0075858619166030259199 & m_{7,8} = -1.4482136587990443235 \\
 m_{3,3} = 1.6154560822068650044 & m_{7,9} = \frac{3}{20} \\
 m_{3,4} = -1.9194919233346676031 & m_{7,10} = -\frac{1}{90} \\
 m_{3,5} = 1.5610425124000178977 & m_{8,8} = 2.6996599266341938109 \\
 m_{3,6} = -0.90541517327846378866 & m_{8,9} = -\frac{3}{2} \\
 m_{3,7} = 0.29650034382549239075 & m_{8,10} = \frac{3}{20} \\
 m_{3,8} = -0.041710318484992597153 & m_{8,11} = -\frac{1}{90}
 \end{array}$$

In the interior we have the symmetric scheme: $-h(Mv)_j = -\frac{1}{560}v_{j-4} + \frac{8}{315}v_{j-3} - \frac{1}{5}v_{j-2} + \frac{8}{5}v_{j-1} - \frac{205}{72}v_j + \frac{8}{5}v_{j+1} - \frac{1}{5}v_{j+2} + \frac{8}{315}v_{j+3} - \frac{1}{560}v_{j+4}$. The fourth-order accurate

boundary derivative operator is given by:

$$BS = \begin{bmatrix} \frac{12700800}{7493827} & -\frac{1009703933}{449629620} & \frac{2502175}{44962962} & \frac{913407}{1362514} & \frac{8487881}{44962962} & -\frac{49651253}{89925924} & \frac{7048944}{37469135} \\ & & 0 & & & & \\ & & & & \ddots & & \\ & & & & & & \end{bmatrix}$$

REFERENCES

- CALABRESE, G. 2005 Finite differencing second order systems describing black holes. *Physical Review D* **71**, 027501.
- CARPENTER, M. H., GOTTLIEB, D. & ABARBANEL, S. 1994 Time-stable boundary conditions for finite-difference schemes solving hyperbolic systems: Methodology and application to high-order compact schemes. *J. Comp. Phys.* **111**, 220–236.
- FISHER, A.E. & MARSDEN, J.E 1972 The Einstein evolution equations as a first-order quasi-linear symmetric hyperbolic system, I. *Commun. Math. Phys.* **28**, 1–38.
- GUSTAFSSON, B., KREISS, H.-O. & SUNDSTRÖM, A. 1972 Stability theory of difference approximations for mixed initial boundary value problems. *Math. Comp.* **26**, 649–686.
- HAM, F., MATTSSON, K. & IACCARINO, G. 2007 Accurate and stable finite volume operators for unstructured flow solvers. *Annual Research Briefs 2006* Center for Turbulence Research, Stanford University, NASA Ames, 243–261.
- KREISS, H.-O. & SCHERER, G. 1974 Finite element and finite difference methods for hyperbolic partial differential equations. *Mathematical Aspects of Finite Elements in Partial Differential Equations.*, Academic Press, Inc.
- KREISS, H.-O., PETERSSON, N. A. & YSTRÖM, J. 2002 Difference approximations for the second order wave equation. *SIAM J. Num. Anal.* **40**, 1940–1967.
- LELE, S. K. 1992 Compact Finite Difference Schemes with Spectral-like Resolution. *J. Comp. Phys.* **103**, 16–42.
- MATTSSON, K., SVÄRD, M. & NORDSTRÖM, J. 2004 Stable and Accurate Artificial Dissipation. *J. Sci. Comput.* **21**, 57–79.
- MATTSSON, K. & NORDSTRÖM, J. 2004 Summation by parts operators for finite difference approximations of second derivatives. *J. Comp. Phys.* **199**, 503–540.
- MATTSSON, K. & NORDSTRÖM, J. 2006 High order finite difference methods for wave propagation in discontinuous media. *J. Comp. Phys.* **220**, 249–269.
- NORDSTRÖM, J., VAN DER WEIDE, E. & GONG, J. 2008 A hybrid method for the unsteady compressible Navier-Stokes equations. *Annual Research Briefs 2007*. Center for Turbulence Research, Stanford University, NASA Ames.
- STRAND, B. 1994 Summation by parts for finite difference approximations for d/dx. *J. Comp. Phys.* **110**, 47–67.
- SZILAGYL, B., KREISS, H.-O. & WINICOUR, J.W. 2005 Modeling the black hole excision problem. *Physical Review D* **71**, 104035.